PERGAMON

International Journal of Solids and Structures 40 (2003) 981–999

INTERNATIONAL JOURNAL OF SOLIDS and STRUCTURES

www.elsevier.com/locate/ijsolstr

A mechanics-of-materials model for predicting Young's modulus of damaged woven fabric composites involving three damage modes

X.-L. Gao [a,*], K. Li [a], S. Mall [b]

[a] *Department of Mechanical Engineering-Engineering Mechanics, Michigan Technological University, 1400 Townsend Drive, Houghton, MI 49931-1295, USA*

[b] *Materials and Manufacturing Directorate, Air Force Research Laboratory, 2230 Tenth Street, Wright-Patterson Air Force Base, OH 45433-7817, USA*

Received 17 October 2001; received in revised form 7 October 2002

Abstract

An analytical model for damaged woven fabric composites is developed using the theory of advanced mechanics of materials. The analysis is based on Castigliano's second theorem and utilizes a damaged mosaic model laminate. Three damage modes (i.e., transverse yarn cracking, interface debonding, and sliding with friction at the interface) are considered. Only one independent interfacial parameter, the friction coefficient between warp and fill yarns, is introduced in the analysis. A closed-form formula is provided for estimating effective Young's modulus of damaged woven laminates. A parametric study of some 192 sample cases of two different composite systems (i.e., glass fiber/epoxy and ceramic fiber/ceramic) is conducted to illustrate the application and significance of the newly derived analytical model. The numerical values of the effective Young's modulus for the special case involving only transverse yarn cracking (the first damage mode) estimated by the present mechanics-of-materials model agree fairly well with those predicted by an elasticity-based model [Int. J. Solids Struct. 38 (2001) 855]. For the general case involving all three damage modes simultaneously, the present model reveals the complex nature of Young's modulus reduction in a quantitative manner, which differs from existing models.

Keywords: Woven fabric composites; Damage modeling; Effective Young's modulus; Energy method; Homogenization theory; Transverse yarn cracking; Interface debonding; Sliding with friction

1. Introduction

In the last three decades the "high-tech" composites based on unidirectional continuous fiber-reinforced laminates, together with the "high-volume" composites reinforced by short fibers or particulates, have been

* Corresponding author. Tel.: +1-906-487-1898; fax: +1-906-487-2822.
E-mail address: xgao@mtu.edu (X.-L. Gao).

0020-7683/02/$ - see front matter © 2002 Elsevier Science Ltd. All rights reserved.
PII: S0020-7683(02)00603-0

thoroughly studied and successfully applied in many industries including construction, transportation and manufacturing. However, limited research has been conducted on fabric-reinforced composites, often called textile composites, partially due to the complexities of their microstructures and the difficulties in modeling them.

Textile (including woven, braided and knitted) composites are produced by impregnating dry fabric preforms with a matrix material through a chemical/physical process. A reinforcing fabric preform is mechanically made by interlacing two or more sets of (orthogonal) fiber bundles (yarns) according to a given weaving/braiding/knitting pattern. Since the number of possible fabric preforms is virtually unlimited, textile composites offer a great potential for tailored (optimal) designs and increased applications. Specifically, such composites have the following major advantages over unidirectional laminate composites: (1) the handling is easier and the fabrication cost could be lower, since the state-of-the-art weaving equipment existing in textile industries can be adapted/used; (2) the delamination problem can be solved by using suitable three-dimensional preform manufacturing processes; (3) the through-thickness strength is higher and the impact resistance is improved; (4) thick textile composites are easier to produce; (5) three-dimensional structural components of composites can be produced without using joints. These merits have made textile composites very attractive in structural applications. For instance, the horizontal stabilizers of Boeing 737 airplane were built using woven fabric composites (McCarty et al., 1982), and about 25% of the composite components used in F22 Aircraft were made from woven fabric composites (Roy, 1998a).

On the other hand, the interlacing and undulations of fiber yarns and the interactions between yarns and matrix make the geometrical modeling of textile composites alone very difficult. The situation is even worse for stress analyses and/or damage modeling. Most publications on textile composites have been devoted to predictions and/or measurements of their thermo-elastic properties (see, for example, Tan et al., 1997; Gao and Mall, 2000). Very few studies have been reported on modeling of damaged/cracked textile composites, and, as a result, the failure mechanisms of such composites are still not well understood.

Because of their highly complex microstructures, even woven composites, the simplest form of textile composites, are very difficult to characterize either experimentally or analytically. This necessitates approximations/simplifications of various kinds in their modeling. For example, three one-dimensional models (i.e., mosaic, crimp and bridging) were developed using the classical laminate theory to estimate material properties of woven composites analytically (Chou and Ishikawa, 1989), and a cross-ply laminate model was used to simulate the behavior of a cracked plain-weave ceramic matrix composite (Birman and Byrd, 1999). Also, special cross-ply laminates were constructed and used as "model laminates" to study the failure mechanisms of woven composites experimentally (Roy, 1998b). More recently, a cracked mosaic model was proposed to predict stress distributions in and effective Young's modulus of damaged woven composites (Gao and Mall, 2001).

The objective of this paper is to present a simple mechanistic model for estimating effective Young's modulus of damaged woven composites using the theory of advanced mechanics of materials. This model is based on Castigliano's second theorem in structural mechanics, as opposed to the previous analysis by Gao and Mall (2001) built on the minimum complementary energy principle in continuum mechanics. The current analysis is a first attempt at modeling damaged woven composites using principles of mechanics of materials and concepts of structural analysis. The rest of this paper is organized as follows. In Section 2, the equilibrium analysis of the mechanics-of-materials type is carried out to solve for the resultant forces in each block of an identified unit cell. Castigliano's second theorem is applied in Section 3 to derive the load–displacement relation on the unit cell level. In Section 4, this resulting relation is utilized in the context of composite homogenization theory to obtain a closed-form formula for calculating the effective Young's modulus of the damaged laminate. Numerical results for sample cases are provided in Section 5 to illustrate the application and significance of the new model. A summary is given in the sixth and last section.

2. Equilibrium analysis

It has been known from experimental studies (Morvan and Baste, 1998; Gao et al., 1999) that possible damage modes for planar woven fabric composites under uniaxial tensile loading include cracking of transverse yarns, interface debonding, sliding with friction at the interface, longitudinal yarn cracking, and fiber–matrix sliding inside longitudinal yarns. Transverse yarn cracking, as the first observable type of damage in woven composites such as SiC/SiC (Morvan and Baste, 1998), graphite/epoxy (Roy, 1998b) and carbon/polyimide (Gao et al., 1999), has been recently analyzed by Gao and Mall (2001) using the principle of minimum complementary energy. As a first step toward modeling of the damaged woven composites based on three-dimensional elasticity theory, the analysis of Gao and Mall (2001) considered only the first damage mode and used a mosaic laminate model. As a natural extension of that analysis, the present model, also utilizing a mosaic laminate, deals with the first three damage modes mentioned above.

Consider a uniaxially loaded woven laminate with the out-of-phase stacking configuration and involving three damage modes, as shown in Fig. 1. Based on the experimental observations of Roy (1998b) and Gao et al. (1999), it is assumed that the cracks in transverse yarns are of the through-thickness type and are, as a first approximation, uniformly located in the middle of each transverse yarn. The second and third damage modes, i.e., interface debonding and sliding with friction at the interface, will be characterized through enforcing interface traction continuity conditions and invoking appropriate interfacial constitutive relations.

In addition, we assume that the laminate is in the plane stress state in the width direction and that the warp and fill yarns are identical orthotropic (or transversely isotropic) materials. Then, from symmetry and periodicity only the repeating unit illustrated in Fig. 2, which is also identified in Fig. 1 using dashed lines, needs to be analyzed. It has the length L, height h and width 1, as shown in Fig. 2, where L_c is the debonded

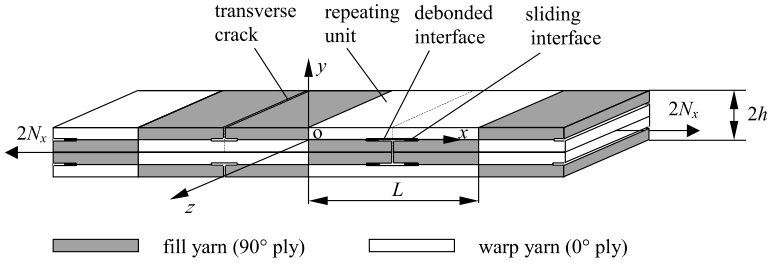

Fig. 1. Woven laminate with cracked transverse yarns and damaged interfaces.

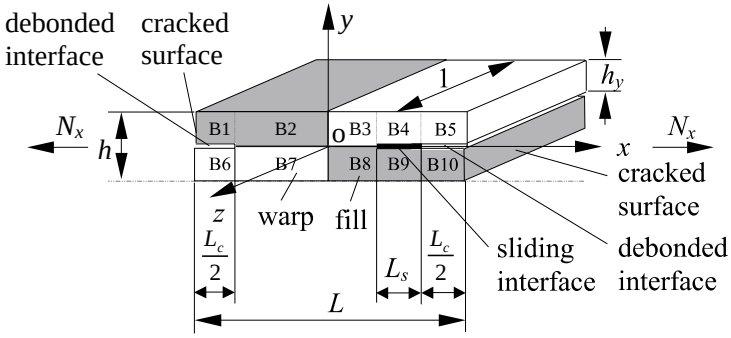

Fig. 2. Repeating unit.

length and L_s is the sliding length, both along the interface $y = 0$. Note that L_c and L_s can be adjusted independently as long as $L_c/2 + L_s \leqslant L/2$ is satisfied. It is pointed out that the way of treating the sliding zone as extended from a debonded zone on the interface here is similar to what was done by Tandon and Pagano (1996) in modeling damaged unidirectional brittle matrix composites.

Aiming at developing a simple mechanistic model, we will be primarily using concepts of structural analysis and principles of advanced mechanics of materials. It is assumed that the repeating unit shown in Fig. 2 can be decomposed into 10 blocks (structural members), each of which can deform independently. The adjacent blocks are linked to each other through the traction/resultant force continuity conditions at the yarn and block interfaces. The constant resultant forces in Blocks 1, 5, 6 and 10, which are obtained here by inspection, can also be rigorously determined from the equilibrium equations and the boundary conditions using the elasticity theory, as was done by Gao and Li (2002) in a separate analysis of a relevant problem. The free body diagrams of the differential elements of the remaining six blocks are illustrated in Fig. 3. Based on these free body diagrams, standard equilibrium analyses of the mechanics-of-materials type can be carried out for each block by enforcing $\sum F_x = 0$, $\sum F_y = 0$ and $\sum M_z = 0$, where the subscripts x, y and z represent the three axes of the Cartesian coordinate system, with z being the out-of-plane axis (see Fig. 2). The results of such analyses are given in the following.

For Block 1, which is traction-free on its top, bottom and left surfaces (see Fig. 2), the resultant forces are, by inspection,

$$N_1 = Q_1 = M_1 = 0. \tag{1}$$

For Block 5, which is traction-free on its top and bottom surfaces and subjected to N_x on its right surface (see Fig. 2), the resultant forces are, by inspection,

$$N_5 = N_x, \qquad Q_5 = M_5 = 0, \tag{2}$$

where N_x is the external load in the x-direction. For Block 6, which is traction-free on its top surface, shear-free on its bottom surface and subjected to N_x on its left surface (see Fig. 2), the resultant forces are, by inspection,

$$N_6 = N_x, \qquad Q_6 = M_6 = 0. \tag{3}$$

For Block 10, which is traction-free on its top and right surfaces and shear-free on its bottom surface (see Fig. 2), the resultant forces are, by inspection,

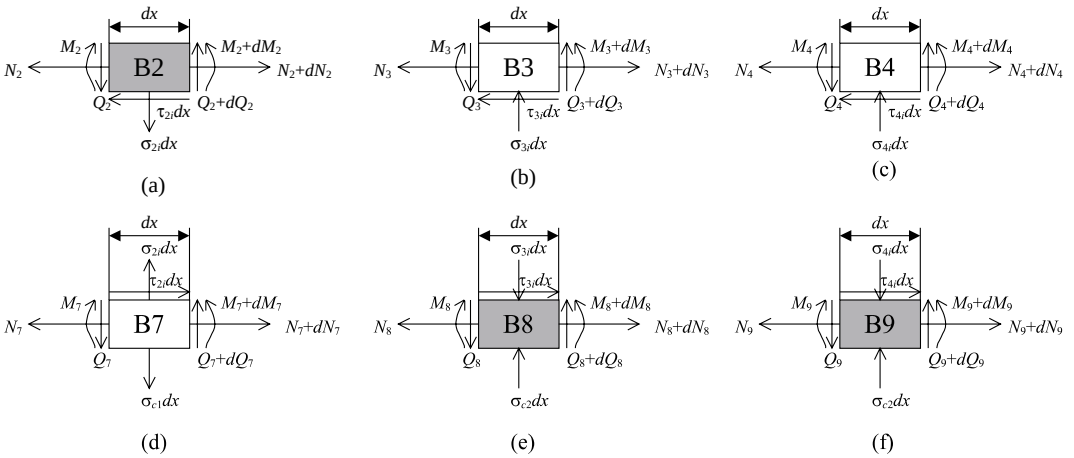

Fig. 3. Free body diagrams.

$$N_{10} = Q_{10} = M_{10} = 0. \tag{4}$$

For Block 2 (see Fig. 3a),

$$\tau_{2i} = \frac{\mathrm{d}N_2}{\mathrm{d}x}, \quad \sigma_{2i} = \frac{\mathrm{d}Q_2}{\mathrm{d}x}, \quad Q_2 - \frac{\tau_{2i}h}{4} = -\frac{\mathrm{d}M_2}{\mathrm{d}x}, \tag{5a, b, c}$$

where σ_{2i}, τ_{2i} are, respectively, the normal and tangential stress components acting on the interface between Blocks 2 and 7, and N_2, Q_2 and M_2 are, respectively, the normal force, shear force and bending moment (i.e., resultant forces) in Block 2. The subscript "i" in Eqs. (5a,b,c) and in the sequel stands for "interface". The resultant force continuity conditions on $x = -(L - L_c)/2$ (see Fig. 2) require that

$$N_2|_{x=-\frac{L-L_c}{2}} = 0, \quad Q_2|_{x=-\frac{L-L_c}{2}} = 0, \quad M_2|_{x=-\frac{L-L_c}{2}} = 0, \tag{6a, b, c}$$

where use has been made of Eq. (1). For Block 3 (see Fig. 3b),

$$\tau_{3i} = \frac{\mathrm{d}N_3}{\mathrm{d}x}, \quad \sigma_{3i} = -\frac{\mathrm{d}Q_3}{\mathrm{d}x}, \quad Q_3 - \frac{\tau_{3i}h}{4} = -\frac{\mathrm{d}M_3}{\mathrm{d}x}, \tag{7a, b, c}$$

where σ_{3i}, τ_{3i} are, respectively, the normal and tangential stress components acting on the interface between Blocks 3 and 8, and N_3, Q_3 and M_3 are the resultant forces in Block 3. The continuity conditions on $x = 0$ (see Fig. 2) are

$$N_3|_{x=0} = N_2|_{x=0}, \quad Q_3|_{x=0} = Q_2|_{x=0}, \quad M_3|_{x=0} = M_2|_{x=0}. \tag{8a, b, c}$$

For Block 4 (see Fig. 3c),

$$\tau_{4i} = \frac{\mathrm{d}N_4}{\mathrm{d}x}, \quad \sigma_{4i} = -\frac{\mathrm{d}Q_4}{\mathrm{d}x}, \quad Q_4 - \frac{\tau_{4i}h}{4} = -\frac{\mathrm{d}M_4}{\mathrm{d}x}, \tag{9a, b, c}$$

where σ_{4i}, τ_{4i} are, respectively, the normal and tangential stress components acting on the interface between Blocks 4 and 9, and N_4, Q_4 and M_4 are the resultant forces in Block 4. The boundary conditions on $x = (L - L_c)/2$ (see Fig. 2) require that

$$N_4|_{x=\frac{L-L_c}{2}} = N_x, \quad Q_4|_{x=\frac{L-L_c}{2}} = 0, \quad M_4|_{x=\frac{L-L_c}{2}} = 0, \tag{10a, b, c}$$

where use has been made of Eq. (2). For Block 7 (see Fig. 3d),

$$\tau_{2i} = -\frac{\mathrm{d}N_7}{\mathrm{d}x}, \quad \sigma_{c1} - \sigma_{2i} = \frac{\mathrm{d}Q_7}{\mathrm{d}x}, \quad Q_7 - \frac{\tau_{2i}h}{4} = -\frac{\mathrm{d}M_7}{\mathrm{d}x}, \tag{11a, b, c}$$

where σ_{c1} is the normal stress component acting on Block 7 at the middle plane $x = -h/2$, and N_7, Q_7 and M_7 are the resultant forces in Block 7. The resultant force continuity conditions on $x = -(L - L_c)/2$ are

$$N_7|_{x=-\frac{L-L_c}{2}} = N_x, \quad Q_7|_{x=-\frac{L-L_c}{2}} = 0, \quad M_7|_{x=-\frac{L-L_c}{2}} = 0, \tag{12a, b, c}$$

where use has been made of Eq. (3). For Block 8 (see Fig. 3e),

$$\tau_{3i} = -\frac{\mathrm{d}N_8}{\mathrm{d}x}, \quad \sigma_{c2} - \sigma_{3i} = -\frac{\mathrm{d}Q_8}{\mathrm{d}x}, \quad Q_8 - \frac{\tau_{3i}h}{4} = -\frac{\mathrm{d}M_8}{\mathrm{d}x}, \tag{13a, b, c}$$

where σ_{c2} is the normal stress component acting on Blocks 8 and 9 at the middle plane $y = -h/2$, and N_8, Q_8 and M_8 are the resultant forces in Block 8. The continuity conditions on $x = 0$ require that

$$N_8|_{x=0} = N_7|_{x=0}, \quad Q_8|_{x=0} = Q_7|_{x=0}, \quad M_8|_{x=0} = M_7|_{x=0}. \tag{14a, b, c}$$

For Block 9 (see Fig. 3f),

$$\tau_{4i} = -\frac{\mathrm{d}N_9}{\mathrm{d}x}, \quad \sigma_{c2} - \sigma_{4i} = -\frac{\mathrm{d}Q_9}{\mathrm{d}x}, \quad Q_9 - \frac{\tau_{4i}h}{4} = -\frac{\mathrm{d}M_9}{\mathrm{d}x}, \tag{15a, b, c}$$

where N_9, Q_9 and M_9 are the resultant forces in Block 9. The resultant force continuity conditions on $x = (L - L_c)/2$ (see Fig. 2) are

$$N_9|_{x=\frac{L-L_c}{2}} = 0, \quad Q_9|_{x=\frac{L-L_c}{2}} = 0, \quad M_9|_{x=\frac{L-L_c}{2}} = 0, \tag{16a, b, c}$$

where use has been made of Eq. (4). Finally, the continuity conditions on $x = (L - L_c)/2 - L_s$ require that

$$N_3|_{x=\frac{L-L_c}{2}-L_s} = N_4|_{x=\frac{L-L_c}{2}-L_s}, \quad Q_3|_{x=\frac{L-L_c}{2}-L_s} = Q_4|_{x=\frac{L-L_c}{2}-L_s}, \quad M_3|_{x=\frac{L-L_c}{2}-L_s} = M_4|_{x=\frac{L-L_c}{2}-L_s}, \tag{17a, b, c}$$

and

$$N_8|_{x=\frac{L-L_c}{2}-L_s} = N_9|_{x=\frac{L-L_c}{2}-L_s}, \quad Q_8|_{x=\frac{L-L_c}{2}-L_s} = Q_9|_{x=\frac{L-L_c}{2}-L_s}, \quad M_8|_{x=\frac{L-L_c}{2}-L_s} = M_9|_{x=\frac{L-L_c}{2}-L_s}. \tag{18a, b, c}$$

Clearly, all equilibrium equations, boundary conditions and interface continuity conditions have already been enforced in the context of mechanics of materials to derive the mathematical expressions presented above. In particular, the effects of transverse (fill) yarn cracking (i.e., the first damage mode) and interface debonding (i.e., the second damage mode) have been incorporated through enforcing the traction-free boundary conditions as reflected in Eqs. (1)–(4). Sliding with friction at the interface, which corresponds to the third damage mode, needs to be characterized by using appropriate interfacial constitutive laws. Along the line of Gao et al. (1988), it is assumed that the interfacial shear stress τ_{4i} on the sliding interface is related to the interfacial normal stress (pressure) σ_{4i} by

$$\tau_{4i} = \mu\sigma_{4i}, \tag{19}$$

where μ is the friction coefficient along the interface. For σ_{4i}, a linear slip-softening model (see, for example, Bao and Song, 1993) is adopted, i.e.,

$$\sigma_{4i} = D\left(\frac{L - L_c}{2} - x\right), \tag{20}$$

where D is a constant parameter representing the degree of damage of the sliding interface. Mathematically, D is the linear rate of change (i.e., the slope) of σ_{4i} with respect to x (see Fig. 5). This parameter is determinable from given geometry and applied load, as will be shown near the end of this section.

Integrating Eqs. (5a,b,c) and using Eq. (6a,b,c) will lead to

$$\begin{aligned} N_2(x) &= \tau_{2i}\left(x + \frac{L - L_c}{2}\right), \\ Q_2(x) &= \sigma_{2i}\left(x + \frac{L - L_c}{2}\right), \\ M_2(x) &= -\frac{\sigma_{2i}}{2}\left(x + \frac{L - L_c}{2}\right)^2 + \frac{\tau_{2i}h}{4}\left(x + \frac{L - L_c}{2}\right). \end{aligned} \tag{21a, b, c}$$

From Eqs. (7a,b,c), (8a,b,c) and (21a,b,c) it follows that

$$\begin{aligned} N_3(x) &= \tau_{3i}x + \tau_{2i}\left(\frac{L - L_c}{2}\right), \\ Q_3(x) &= -\sigma_{3i}x + \sigma_{2i}\left(\frac{L - L_c}{2}\right), \\ M_3(x) &= \frac{\sigma_{3i}}{2}x^2 - \left[\sigma_{2i}\left(\frac{L - L_c}{2}\right) - \frac{\tau_{3i}h}{4}\right]x - \frac{\sigma_{2i}}{2}\left(\frac{L - L_c}{2}\right)^2 + \frac{\tau_{2i}h}{4}\left(\frac{L - L_c}{2}\right). \end{aligned} \tag{22a, b, c}$$

Using Eqs. (9a,b,c), (10a,b,c), (19) and (20) gives

$$\begin{aligned} N_4(x) &= -\frac{1}{2}\mu D\left(\frac{L-L_c}{2}-x\right)^2 + N_x, \\ Q_4(x) &= \frac{1}{2}D\left(\frac{L-L_c}{2}-x\right)^2, \\ M_4(x) &= \frac{1}{2}D\left(\frac{L-L_c}{2}-x\right)^2\left[-\frac{h}{4}\mu+\frac{1}{3}\left(\frac{L-L_c}{2}-x\right)\right]. \end{aligned} \tag{23a, b, c}$$

From Eqs. (11a,b,c) and (12a,b,c) one obtains

$$\begin{aligned} N_7(x) &= -\tau_{2i}\left(x+\frac{L-L_c}{2}\right)+N_x, \\ Q_7(x) &= (\sigma_{c1}-\sigma_{2i})\left(x+\frac{L-L_c}{2}\right), \\ M_7(x) &= -\frac{(\sigma_{c1}-\sigma_{2i})}{2}\left(x+\frac{L-L_c}{2}\right)^2+\frac{\tau_{2i}h}{4}\left(x+\frac{L-L_c}{2}\right). \end{aligned} \tag{24a, b, c}$$

The use of Eqs. (13a,b,c), (14a,b,c) and (24a,b,c) results in

$$\begin{aligned} N_8(x) &= -\tau_{3i}x-\tau_{2i}\left(\frac{L-L_c}{2}\right)+N_x, \\ Q_8(x) &= -(\sigma_{c2}-\sigma_{3i})x+(\sigma_{c1}-\sigma_{2i})\left(\frac{L-L_c}{2}\right), \\ M_8(x) &= \frac{(\sigma_{c2}-\sigma_{3i})}{2}x^2-\left[(\sigma_{c1}-\sigma_{2i})\left(\frac{L-L_c}{2}\right)-\frac{\tau_{3i}h}{4}\right]x-\frac{(\sigma_{c1}-\sigma_{2i})}{2}\left(\frac{L-L_c}{2}\right)^2+\frac{\tau_{2i}h}{4}\left(\frac{L-L_c}{2}\right). \end{aligned} \tag{25a, b, c}$$

It follows from Eqs. (15a,b,c), (16a,b,c), (19) and (20) that

$$\begin{aligned} N_9(x) &= \frac{1}{2}\mu D\left(\frac{L-L_c}{2}-x\right)^2, \\ Q_9(x) &= -\frac{1}{2}D\left(\frac{L-L_c}{2}-x\right)^2+\sigma_{c2}\left(\frac{L-L_c}{2}-x\right), \\ M_9(x) &= \frac{1}{2}\left(\frac{L-L_c}{2}-x\right)^2\left[\sigma_{c2}-\frac{h}{4}\mu D-\frac{1}{3}D\left(\frac{L-L_c}{2}-x\right)\right]. \end{aligned} \tag{26a, b, c}$$

Using Eqs. (22a) and (23a) in Eq. (17a) gives

$$\tau_{3i}\left(\frac{L-L_c}{2}-L_s\right)+\tau_{2i}\left(\frac{L-L_c}{2}\right)+\frac{1}{2}\mu D L_s^2 = N_x. \tag{27}$$

The global equilibrium of the repeating unit (see Fig. 4) requires that

$$-\sigma_{c1}\left(\frac{L-L_c}{2}\right)+\sigma_{c2}\left(\frac{L-L_c}{2}\right)=0, \quad -\int_{-\frac{L-L_c}{2}}^{0}\sigma_{c1}x\,dx+\int_{0}^{\frac{L-L_c}{2}}\sigma_{c2}x\,dx = 4\int_0^{h/2}\frac{N_x}{h}y\,dy, \tag{28a, b}$$

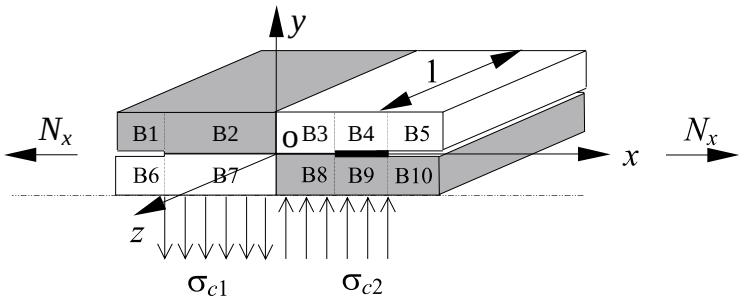

Fig. 4. Global equilibrium of the repeating unit.

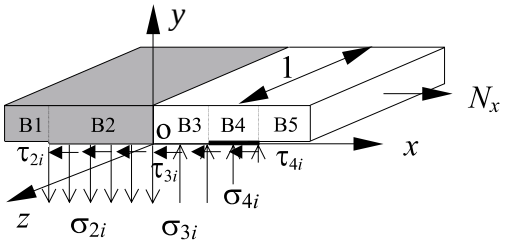

Fig. 5. Global equilibrium of Blocks 1–5.

which gives

$$\sigma_{c1} = \sigma_{c2} = \frac{2N_x h}{(L - L_c)^2}. \tag{29}$$

The continuity of the normal interfacial stress at $x = (L - L_c)/2 - L_s$ (see Figs. 2 and 5) yields, using Eq. (20),

$$\sigma_{3i} = DL_s. \tag{30}$$

Also, the global equilibrium of Blocks 1–5 (see Fig. 5) requires that

$$\begin{aligned} &\sigma_{2i}\left(\frac{L - L_c}{2}\right) = \sigma_{3i}\left(\frac{L - L_c}{2} - L_s\right) + \frac{1}{2}\sigma_{3i}L_s, \\ &-\int_{-\frac{L-L_c}{2}}^{0} \sigma_{2i}x\,dx + \int_{0}^{\frac{L-L_c}{2}-L_s} \sigma_{3i}x\,dx + \int_{\frac{L-L_c}{2}-L_s}^{\frac{L-L_c}{2}} D\left(\frac{L - L_c}{2} - x\right)x\,dx - 2\int_{0}^{h/2} \frac{N_x}{h}y\,dy = 0. \end{aligned} \tag{31a, b}$$

The solution of Eqs. (31a,b) gives

$$\sigma_{3i} = \frac{6N_x h}{6L^2 - 9LL_s - 12LL_c + 9L_cL_s + 6L_c^2 + 4L_s^2}, \qquad \sigma_{2i} = \frac{\sigma_{3i}(L - L_c - L_s)}{L - L_c}. \tag{32a, b}$$

To simplify the model, it is further assumed that $\tau_{2i} = \tau_{3i}$. Substituting this and Eq. (30) into Eq. (27) leads to

$$\tau_{2i} = \frac{N_x - \frac{1}{2}\mu L_s\sigma_{3i}}{L - (L_s + L_c)}. \tag{33}$$

Note that we have obtained explicit expressions for the resultant forces in all of the 10 blocks in terms of the external load N_x, given material properties and geometrical constants, and the identified interfacial parameters μ and D. In fact, D can be obtained from Eqs. (30) and (32a) in terms of the applied load and the unit cell geometry as

$$D = \frac{1}{L_s}\frac{6N_x h}{6L^2 - 9LL_s - 12LL_c + 9L_cL_s + 6L_c^2 + 4L_s^2}. \tag{34}$$

This shows that D is a non-zero constant for given $N_x \neq 0$ and $L < \infty$. Hence, only one independent interfacial (constitutive) parameter, μ, is involved in this model.

3. Load–displacement relation

In the preceding section, the resultant forces in each of the 10 blocks of the repeating unit have been determined. In order to obtain the effective Young's modulus of the damaged woven laminate, one only needs to derive the stress–strain relation on the repeating unit level. Equivalently, it will be sufficient to have the load–displacement relation known for the repeating unit that is subjected to uniaxial loading in the x-direction (see Fig. 2). This can be done efficiently by using Castigliano's second theorem in structural analysis (see, for example, Cook and Young, 1999). As an energy principle, this theorem allows one to work with scalars (and to use local coordinate systems).

Note that the total complementary energy of the repeating unit is given by

$$\Pi_c = \sum_{j=1}^{10} \Pi_j, \tag{35}$$

where Π_j is the complementary energy in the jth block. For Block 1,

$$\Pi_1 = \int_{-\frac{L}{2}}^{-\frac{L-L_c}{2}} \left(\frac{N_1}{2}\frac{N_1\,dx}{E_2A} + \frac{M_1}{2}\frac{M_1\,dx}{E_2I} + \frac{Q_1}{2}\frac{kQ_1\,dx}{G_{23}A} \right), \tag{36}$$

where the cross-sectional area $A = h/2$, the moment of area $I = h^3/96$, and the transverse shear factor $k = 1.2$ (Cook and Young, 1999). For Block 2,

$$\Pi_2 = \int_{-\frac{L-L_c}{2}}^{0} \left(\frac{N_2}{2}\frac{N_2\,dx}{E_2A} + \frac{M_2}{2}\frac{M_2\,dx}{E_2I} + \frac{Q_2}{2}\frac{kQ_2\,dx}{G_{23}A} \right). \tag{37}$$

For Block 3,

$$\Pi_3 = \int_{0}^{\frac{L-L_c}{2}-L_s} \left(\frac{N_3}{2}\frac{N_3\,dx}{E_1A} + \frac{M_3}{2}\frac{M_3\,dx}{E_1I} + \frac{Q_3}{2}\frac{kQ_3\,dx}{G_{13}A} \right). \tag{38}$$

For Block 4,

$$\Pi_4 = \int_{\frac{L-L_c}{2}-L_s}^{\frac{L-L_c}{2}} \left(\frac{N_4}{2}\frac{N_4\,dx}{E_1A} + \frac{M_4}{2}\frac{M_4\,dx}{E_1I} + \frac{Q_4}{2}\frac{kQ_4\,dx}{G_{13}A} \right). \tag{39}$$

For Block 5,

$$\Pi_5 = \int_{\frac{L-L_c}{2}}^{\frac{L}{2}} \left(\frac{N_5}{2}\frac{N_5\,dx}{E_1A} + \frac{M_5}{2}\frac{M_5\,dx}{E_1I} + \frac{Q_5}{2}\frac{kQ_5\,dx}{G_{13}A} \right). \tag{40}$$

For Block 6,

$$\Pi_6 = \int_{-\frac{L}{2}}^{-\frac{L-L_c}{2}} \left(\frac{N_6}{2} \frac{N_6\,\mathrm{d}x}{E_1 A} + \frac{M_6}{2} \frac{M_6\,\mathrm{d}x}{E_1 I} + \frac{Q_6}{2} \frac{kQ_6\,\mathrm{d}x}{G_{13}A} \right). \tag{41}$$

For Block 7,

$$\Pi_7 = \int_{-\frac{L-L_c}{2}}^{0} \left(\frac{N_7}{2} \frac{N_7\,\mathrm{d}x}{E_1 A} + \frac{M_7}{2} \frac{M_7\,\mathrm{d}x}{E_1 I} + \frac{Q_7}{2} \frac{kQ_7\,\mathrm{d}x}{G_{13}A} \right). \tag{42}$$

For Block 8,

$$\Pi_8 = \int_{0}^{\frac{L-L_c}{2}-L_s} \left(\frac{N_8}{2} \frac{N_8\,\mathrm{d}x}{E_2 A} + \frac{M_8}{2} \frac{M_8\,\mathrm{d}x}{E_2 I} + \frac{Q_8}{2} \frac{kQ_8\,\mathrm{d}x}{G_{23}A} \right). \tag{43}$$

For Block 9,

$$\Pi_9 = \int_{\frac{L-L_c}{2}-L_s}^{\frac{L-L_c}{2}} \left(\frac{N_9}{2} \frac{N_9\,\mathrm{d}x}{E_2 A} + \frac{M_9}{2} \frac{M_9\,\mathrm{d}x}{E_2 I} + \frac{Q_9}{2} \frac{kQ_9\,\mathrm{d}x}{G_{23}A} \right). \tag{44}$$

Finally, for Block 10,

$$\Pi_{10} = \int_{\frac{L-L_c}{2}}^{\frac{L}{2}} \left(\frac{N_{10}}{2} \frac{N_{10}\,\mathrm{d}x}{E_2 A} + \frac{M_{10}}{2} \frac{M_{10}\,\mathrm{d}x}{E_2 I} + \frac{Q_{10}}{2} \frac{kQ_{10}\,\mathrm{d}x}{G_{23}A} \right). \tag{45}$$

Note that E_α and $G_{\alpha 3} (\alpha \in \{1,2\})$ in Eqs. (36)–(45) are material properties with respect to the three principal material axes of warp/fill yarns.

Applying Castigliano's second theorem then gives, from Eq. (35),

$$\Delta_x = \frac{\partial \Pi_c}{\partial N_x} = \sum_{j=1}^{10} \frac{\partial \Pi_j}{\partial N_x}, \tag{46}$$

where Δ_x is the displacement of the repeating unit in the loading direction. By using Eqs. (1)–(4) and (21a,b,c)–(26a,b,c) in Eqs. (36)–(45), $\partial \Pi_j / \partial N_x (j \in \{1,2,\ldots,10\})$ can be explicitly evaluated. The results are provided in Appendix A. The substitution of these results into Eq. (46) will then lead to the final expression of the load–displacement relation $\Delta_x = f(N_x)$.

4. Young's modulus

The effective Young's modulus of the damaged laminate can be determined using the average strain theorem in homogenization theory of composite materials (see, for example, Hashin, 1983). According to this theorem,

$$\varepsilon_x^0 = \overline{\varepsilon_x} \equiv \frac{\Delta_x}{L}, \tag{47}$$

where ε_x^0 is the uniform (constant) strain applied in the longitudinal direction on the homogenized body. Therefore, the effective Young's modulus is given by

$$E_x^* = \frac{\overline{\sigma_x}}{\varepsilon_x^0} = \frac{L}{h} \frac{N_x}{\Delta_x}. \tag{48}$$

Using the functional relationship $\Delta_x = f(N_x)$ derived in the preceding section, one can finally obtain from Eq. (48) that

$$\frac{1}{E_x^*}\frac{L}{h} = \frac{1}{2E_1}\left(\frac{C_{N3}+C_{N4}+C_{N5}+C_{N6}+C_{N7}}{A}+\frac{C_{M3}+C_{M4}+C_{M7}}{I}\right)+\frac{C_{Q3}+C_{Q4}+C_{Q7}}{2G_{13}A} + \frac{1}{2E_2}\left(\frac{C_{N2}+C_{N8}+C_{N9}}{A}+\frac{C_{M2}+C_{M8}+C_{M9}}{I}\right)+\frac{C_{Q2}+C_{Q8}+C_{Q9}}{2G_{23}A}, \tag{49}$$

where constants $C_{N2}-C_{N9}$, $C_{Q2}-C_{Q4}$, $C_{Q7}-C_{Q9}$, $C_{M2}-C_{M4}$ and $C_{M7}-C_{M9}$ are given in Appendix B. By using the closed-form formula given in Eq. (49), the effective Young's modulus of the damaged laminate, E_x^*, can be readily determined.

5. Numerical results

To illustrate the analytical solution derived above, a parametric study of sample cases is carried out in this section. Two unidirectional composites, glass fiber/epoxy and ceramic fiber/ceramic, are used as warp/fill yarn materials in this study. The engineering properties of the two composites, which are regarded as transversely isotropic, are listed in Table 1, where the subscripts 'A' and 'T' stand for axial and transverse directions, respectively. These properties are taken from Hashin (1987) (for the glass fiber/epoxy composite) and Ji et al. (1998) (for the ceramic fiber/ceramic composite).

Some representative numerical values of the effective Young's modulus (E_x^*) are graphically illustrated in Figs. 6–9, which are obtained using Eq. (49). In each case, three values of L/h, which symbolizes the density of cracks in transverse yarns, are considered. Following Gao et al. (1988), $\mu = 0.1$ is taken in the sample calculations. The *Mathematica* program (Wolfram, 1996) is employed in the computation.

Based on the numerical data shown in Figs. 6–9, the following observations can be made:

(1) The effective Young's modulus (E_x^*) estimated by the current mechanics-of-materials model agrees fairly well with that predicted by the more accurate variational solution derived in Gao and Mall (2001). For example, when $L/h = 3$ the two values of E_x^* obtained here for the case with only transverse yarn cracking (that is, $L_c = 0 = L_s$), i.e., 17.47 and 81.35 GPa, are quite close to the two corresponding values (plane stress case) given in Gao and Mall (2001), which are 17.81 and 83.33 GPa, respectively.

(2) The larger L/h is, the larger E_x^* becomes. This is true for all sample cases having different L_c and/or L_s. That is, when the density of transverse yarn cracks (h/L) is smaller, the reduction in Young's modulus is less, regardless of the influences of the second and third damage modes. Also, it is seen that the values of E_x^* corresponding to two neighboring values of L/h are getting closer when L/h becomes larger. These reflect the effects of transverse yarn cracking (i.e., the first damage mode) on the stiffness of the damaged laminate. The trends shown here are the same as those demonstrated by the variational solution of Gao and Mall (2001), where only the first damage mode is considered.

Table 1
Material properties

Property	Glass/epoxy	Ceramic/ceramic
E_A (GPa)	41.7	140.0
E_T (GPa)	13.0	88.0
ν_A	0.30	0.20
ν_T	0.42	0.26
G_A (GPa)	3.40	44.0
G_T (GPa)	4.58	35.0

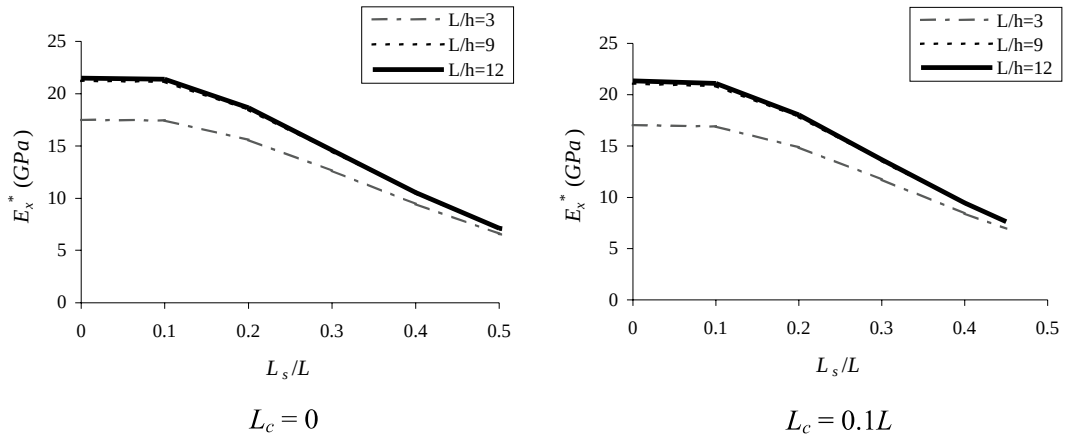

Fig. 6. Young's modulus vs. sliding length: glass/epoxy material.

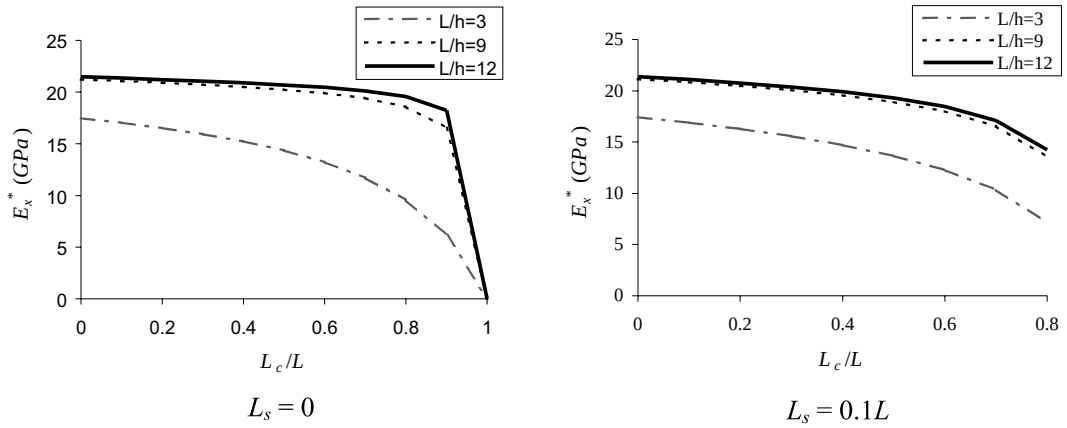

Fig. 7. Young's modulus vs. debonded length: glass/epoxy material.

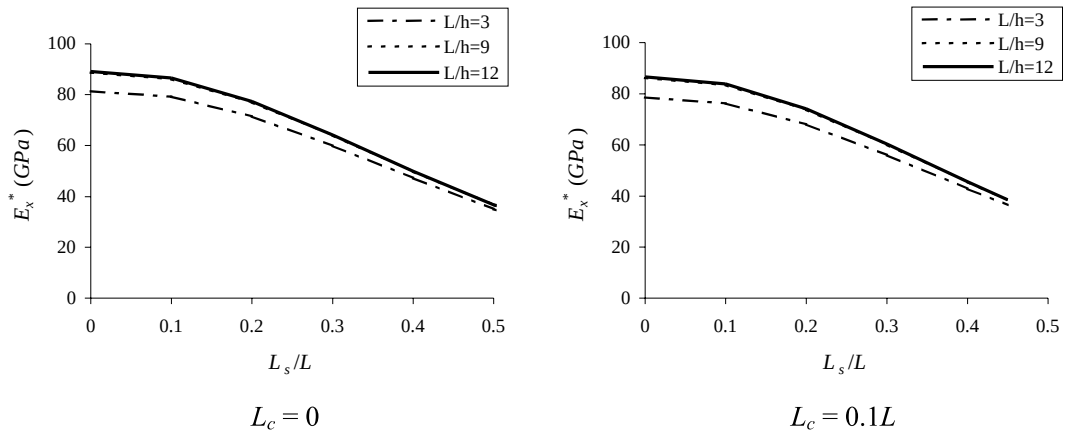

Fig. 8. Young's modulus vs. sliding length: ceramic/ceramic material.

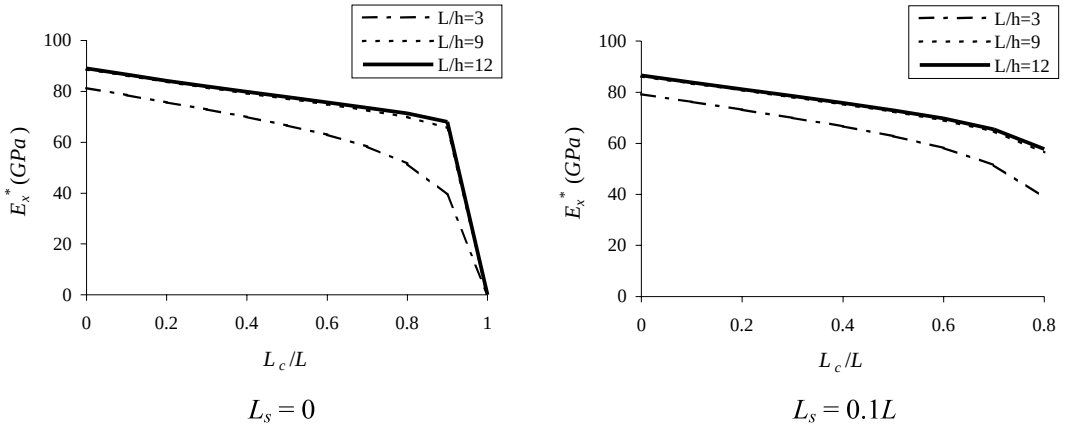

Fig. 9. Young's modulus vs. debonded length: ceramic/ceramic material.

(3) The further reduction in Young's modulus due to interface debonding (in addition to the reduction caused by transverse yarn cracking and interface sliding) appears to be monotonic: the larger the debonded length is, the smaller Young's modulus becomes. This holds for both composite systems, as illustrated in Figs. 7 and 9. The reason for this feature is that progressive debonding along the interface results in the continuous increase of the length of Blocks 1 and 10, which have zero-valued resultant forces and do not store any energy, and thus monotonically reduce the load-carrying capacity of the entire unit cell.

(4) Interface sliding also leads to further reduction in Young's modulus in a monotonic fashion. That is, Young's modulus decreases monotonically with the increase of the sliding length, which is true for all cases considered, as shown in Figs. 6 and 8. This is expected, since a sliding interface (even with friction) is inherently weaker than a perfectly bonded interface (along which the friction coefficient μ is regarded to be infinitely large).

6. Summary

An analytical model is developed for damaged woven fabric composites using a mosaic (woven) laminate. It provides a closed-form formula for calculating the effective Young's modulus of damaged woven laminates. The present analysis is based on Castigliano's second theorem and is of the mechanics-of-materials type. The new model accounts for the first three damage modes observed in a typical woven fabric composite (i.e., transverse yarn cracking, interface debonding, and sliding with friction at the interface), although it contains only one independent interfacial parameter (i.e., the friction coefficient between warp and fill yarns).

The current solution, as a closed-form one, is inherently suitable for parametric studies. A parametric study is performed here for some 192 sample cases using the derived analytical formula. These sample cases involve two different composite systems (used as the yarn materials). When only the first damage mode (i.e., transverse yarn cracking) is present, numerical values of the effective Young's modulus estimated by the current mechanics-of-materials model are in fairly good agreement with those predicted by the elasticity (variational) solution of Gao and Mall (2001). However, when all of the first three damage modes are involved, the situation becomes more complicated, as demonstrated by the numerical results shown in Figs. 6–9. The new analytical model can deal with this situation in a quantitative manner. In contrast, existing analytical models, including that of Gao and Mall (2001), do not have this capability.

As in all other analytical studies, the new model has its own limitations arising from the simplifying assumptions made to facilitate the derivation. For example, the use of a mosaic laminate ignores undulations of fiber yarns, which can be very important for woven composites with large waviness. Nevertheless, with all expressions derived in explicit forms, the current analytical model has an additional use, viz. it can be employed as a benchmark solution to validate computer codes or numerical analyses.

Acknowledgements

The authors wish to thank two anonymous reviewers for their critical and constructive comments on an earlier version of the paper, which have helped to improve the model and its presentation. The financial support of K. Li provided by the Graduate School of the Michigan Technological University is also gratefully acknowledged.

Appendix A

Note that from Eqs. (1) and (36) it follows that

$$\frac{\partial \Pi_1}{\partial N_x} = 0, \tag{A.1}$$

from Eqs. (2) and (40) that

$$\frac{\partial \Pi_5}{\partial N_x} = \frac{L_c N_x}{2E_1 A}, \tag{A.2}$$

from Eqs. (3) and (41) that

$$\frac{\partial \Pi_6}{\partial N_x} = \frac{L_c N_x}{2E_1 A}, \tag{A.3}$$

and from Eqs. (4) and (45) that

$$\frac{\partial \Pi_{10}}{\partial N_x} = 0. \tag{A.4}$$

Using Eqs. (21a,b,c) in Eq. (37) gives

$$\begin{aligned}\frac{\partial \Pi_2}{\partial N_x} = {} & \frac{b_1 \tau_{2i}(L-L_c)^3}{24E_2 A} + \frac{1.2 b_2 \sigma_{2i}(L-L_c)^3}{24G_{23}A} \\ & + \frac{1}{128E_2 I}\left[\frac{b_2\sigma_{2i}(L-L_c)^5}{5} - \frac{h(b_2\tau_{2i}+b_1\sigma_{2i})(L-L_c)^4}{4} + \frac{h^2(L-L_c)^3 b_1 \tau_{2i}}{3}\right],\end{aligned} \tag{A.5}$$

where

$$\begin{aligned} b_1 &\equiv \frac{\partial \tau_{2i}}{\partial N_x} = \frac{\left(1-\frac{1}{2}\mu L_s b_3\right)}{L-(L_s+L_c)}, \qquad b_2 \equiv \frac{\partial \sigma_{2i}}{\partial N_x} = \frac{b_3(L-L_c-L_s)}{L-L_c}, \\ b_3 &\equiv \frac{\partial \sigma_{3i}}{\partial N_x} = \frac{6h}{6L^2 - 9LL_s - 12LL_c + 9L_cL_s + 6L_c^2 + 4L_s^2}. \end{aligned} \tag{A.6}$$

Substituting Eqs. (22a,b,c) into Eq. (38) yields

$$\begin{aligned}\frac{\partial \Pi_3}{\partial N_x} = {} & \frac{b_1\tau_{2i}}{3E_1A}\left[(L-L_c-L_s)^3-\left(\frac{L-L_c}{2}\right)^3\right]+\frac{1}{2G_{13}A}\left(\frac{L-L_c}{2}-L_s\right)\left[\frac{2}{3}b_3\sigma_{3i}\left(\frac{L-L_c}{2}-L_s\right)^2\right.\\ & \left.-\frac{1}{2}(b_2\sigma_{2i}+b_3\sigma_{3i})(L-L_c)\left(\frac{L-L_c}{2}-L_s\right)+2b_2\sigma_{2i}\left(\frac{L-L_c}{2}\right)^2\right]\\ & +\frac{1}{2E_1I}\left\langle\sigma_{3i}\left(\frac{L-L_c}{2}-L_s\right)^3\left\{\left(\frac{L-L_c}{2}-L_s\right)\left[\frac{b_3}{10}\left(\frac{L-L_c}{2}-L_s\right)-\frac{b_2(L-L_c)}{16}+\frac{b_1h}{32}\right]\right.\right.\\ & \left.+\frac{L-L_c}{6}\left[-\frac{b_2(L-L_c)}{8}+\frac{b_1h}{8}\right]\right\}+\frac{1}{2}\sigma_{2i}(L-L_c)\left(\frac{L-L_c}{2}-L_s\right)\left\{\frac{b_3}{8}\left(\frac{L-L_c}{2}-L_s\right)^3\right.\\ & +\frac{1}{3}\left(\frac{L-L_c}{2}-L_s\right)^2\left[b_2(L-L_c)-\frac{b_1h}{2}-\frac{b_3}{8}(L-L_c)\right]+\frac{1}{16}\left(\frac{L-L_c}{2}-L_s\right)(L-L_c)\left[b_2(L-L_c)-\frac{b_1h}{2}\right]\\ & \left.+\frac{L-L_c}{2}\left[\frac{b_2(L-L_c)}{4}-\frac{b_1h}{4}\right]\left[\frac{L-L_c}{2}-\frac{1}{2}\left(\frac{L-L_c}{2}-L_s\right)\right]\right\}\\ & +\tau_{2i}\left(\frac{L-L_c}{2}-L_s\right)\left\{\frac{b_3h}{32}\left(\frac{L-L_c}{2}-L_s\right)^3+\frac{1}{3}\left(\frac{L-L_c}{2}-L_s\right)^2\left[-\frac{b_2h(L-L_c)}{4}+\frac{b_1h^2}{8}+\frac{b_3h(L-L_c)}{16}\right]\right.\\ & -\frac{h}{32}\left(\frac{L-L_c}{2}-L_s\right)(L-L_c)\left[b_2(L-L_c)-\frac{b_1h}{2}\right]-\frac{h}{16}(L-L_c)\left[\frac{b_2}{4}(L-L_c)-\frac{b_1h}{4}\right]\\ & \left.\left.\times\left[\left(\frac{L-L_c}{2}-L_s\right)+2(L-L_c)\right]\right\}\right\rangle. \end{aligned} \tag{A.7}$$

From Eqs. (23a,b,c) and (39) one obtains

$$\frac{\partial \Pi_4}{\partial N_x} = \frac{1}{2E_1A}\left[L_s^3D\left(\frac{b_3\mu^2L_s}{10}-\frac{\mu}{3}\right)+L_sN_x\left(2-\frac{b_3\mu L_s}{3}\right)\right]+\frac{b_3L_s^4D}{20G_{13}A}+\frac{b_3L_s^4D}{4E_1I}\left(\frac{L_s^2}{63}-\frac{h\mu L_s}{36}+\frac{h^2\mu^2}{80}\right). \tag{A.8}$$

Using Eqs. (24a,b,c) in Eq. (42) results in

$$\begin{aligned}\frac{\partial \Pi_7}{\partial N_x} = {} & \frac{1}{2E_1A}\left\{\tau_{2i}\left(\frac{L-L_c}{2}\right)^2\left[\frac{1}{3}b_1(L-L_c)-1\right]+\frac{1}{2}N_x(L-L_c)\left[2-\frac{1}{2}b_1(L-L_c)\right]\right\}\\ & +\frac{1}{24G_{13}A}(b_2-c_1)(\sigma_{2i}-\sigma_{c1})(L-L_c)^3+\frac{1}{16E_1I}(L-L_c)^3\left\{(\sigma_{2i}-\sigma_{c1})\frac{L-L_c}{2}\left[\frac{(b_2-c_1)}{20}(L-L_c)+\frac{b_1h}{16}\right]\right.\\ & \left.+\tau_{2i}\left[\frac{(b_2-c_1)h}{32}(L-L_c)+\frac{b_1h^2}{24}\right]\right\}, \end{aligned} \tag{A.9}$$

where

$$c_1 \equiv \frac{\partial \sigma_{c1}}{\partial N_x} = \frac{2h}{(L-L_c)^2}. \tag{A.10}$$

It follows from Eqs. (25a,b,c) and (43) that

$$\begin{aligned}\frac{\partial \Pi_8}{\partial N_x} = {} & \frac{1}{2E_2A}\left\langle \tau_{2i}\left\{\frac{2}{3}b_1\left[(L-L_s-L_c)^3-\left(\frac{L-L_c}{2}\right)^3\right]-\left[(L-L_s-L_c)^2-\left(\frac{L-L_c}{2}\right)^2\right]\right\}\right. \\ & \left. + N_x\left\{2\left(\frac{L-L_c}{2}-L_s\right)-b_1\left[(L-L_s-L_c)^2-\left(\frac{L-L_c}{2}\right)^2\right]\right\}\right\rangle \\ & + \frac{1}{2G_{23}A}\left\{\left(\frac{L-L_c}{2}-L_s\right)^2(\sigma_{3i}-\sigma_{c2})\left[\frac{2}{3}(b_3-c_2)\left(\frac{L-L_c}{2}-L_s\right)-\frac{1}{2}(b_2-c_1)(L-L_c)\right]\right. \\ & \left. -\frac{1}{2}(\sigma_{2i}-\sigma_{c1})(L-L_c)\left(\frac{L-L_c}{2}-L_s\right)\left[(b_3-c_2)\left(\frac{L-L_c}{2}-L_s\right)-(b_2-c_1)(L-L_c)\right]\right\} \\ & + \frac{1}{2E_1I}\left\langle(\sigma_{3i}-\sigma_{c2})\left(\frac{L-L_c}{2}-L_s\right)^3\left\{\left(\frac{L-L_c}{2}-L_s\right)\left[\frac{b_3}{10}\left(\frac{L-L_c}{2}-L_s\right)-\frac{(b_2-c_1)}{16}(L-L_c)\right.\right.\right. \\ & \left.\left.\left.+\frac{b_1h}{32}\right]+\frac{1}{6}(L-L_c)\left[\frac{(b_2-c_1)}{8}(L-L_c)+\frac{b_1h}{8}\right]\right\}+\frac{1}{2}(\sigma_{2i}-\sigma_{c1})\left(\frac{L-L_c}{2}-L_s\right)(L-L_c)\right. \\ & \times\left\{-(b_3-c_2)\left(\frac{L-L_c}{2}-L_s\right)^2\left[\frac{1}{8}\left(\frac{L-L_c}{2}-L_s\right)+\frac{1}{12}(L-L_c)\right]+\left(\frac{L-L_c}{2}-L_s\right)\right. \\ & \times\left[\frac{1}{2}(b_2-c_1)(L-L_c)+\frac{b_1h}{4}\right]\left[\frac{2}{3}\left(\frac{L-L_c}{2}-L_s\right)+\frac{1}{4}(L-L_c)\right]+\left[\frac{b_2-c_1}{4}(L-L_c)+\frac{b_1h}{4}\right]\frac{L-L_c}{2} \\ & \left.\times\left[\frac{L-L_c}{2}+\frac{1}{2}\left(\frac{L-L_c}{2}-L_s\right)\right]\right\}+\tau_{2i}\left(\frac{L-L_c}{2}-L_s\right) \\ & \times\left\{-\frac{(b_3-c_2)h}{32}\left(\frac{L-L_c}{2}-L_s\right)^3-\frac{h}{6}\left(\frac{L-L_c}{2}-L_s\right)^2\right. \\ & \times\left[-\frac{1}{2}(b_2-c_1)(L-L_c)-\frac{b_1h}{4}+\frac{(b_3-c_2)}{8}(L-L_c)\right] \\ & +\frac{h}{16}\left(\frac{L-L_c}{2}-L_s\right)(L-L_c)\left[\frac{1}{2}(b_2-c_1)(L-L_c)+\frac{b_1h}{4}\right] \\ & \left.+\frac{h}{16}(L-L_c)\left[\frac{b_2}{4}(L-L_c)+\frac{b_1h}{4}\right]\left[\left(\frac{L-L_c}{2}-L_s\right)+2(L-L_c)\right]\right\}\Bigg\rangle, \end{aligned} \tag{A.11}$$

where

$$c_2 \equiv \frac{\partial \sigma_{c2}}{\partial N_x} = \frac{2h}{(L-L_c)^2}. \tag{A.12}$$

Finally, from Eqs. (26a,b,c) and (44) one obtains

$$\begin{aligned}\frac{\partial \Pi_9}{\partial N_x} = {} & \frac{b_3\mu^2L_s^4D}{20E_2A}+\frac{1}{2G_{23}A}\left[DL_s^4\left(\frac{b_3}{10}-\frac{b_2}{4}\right)-\sigma_{c2}L_s^3\left(\frac{b_3}{4}-\frac{2}{3}b_2\right)\right] \\ & +\frac{1}{2E_2I}\left\{2b_3DL_s^4\left(\frac{L_s^2}{252}+\frac{h\mu L_s}{144}+\frac{h^2\mu^2}{320}\right)-L_s^4(b_3\sigma_{c2}+Dc_2L_s)\left(\frac{L_s}{36}+\frac{h\mu}{40}\right)+\frac{c_2\sigma_{c2}}{10}L_s^5\right\}. \end{aligned} \tag{A.13}$$

This completes the evaluation of all $\partial \Pi_j/\partial N_x$ ($j \in \{1,2,\ldots,10\}$), which will be substituted into Eq. (46) to obtain $\Delta_x = f(N_x)$.

Appendix B

The constants $C_{N2}-C_{N9}$, $C_{Q2}-C_{Q4}$, $C_{Q7}-C_{Q9}$, $C_{M2}-C_{M4}$ and $C_{M7}-C_{M9}$ involved in Eq. (49) are given by

$$
\begin{aligned}
&C_{N2}=\frac{2b_1^2}{3}\left(\frac{L-L_c}{2}\right)^3, \qquad C_{Q2}=\frac{2.4b_2^2}{3}\left(\frac{L-L_c}{2}\right)^3,\\
&C_{M2}=\frac{b_2^2}{10}\left(\frac{L-L_c}{2}\right)^5-\frac{hb_1b_2}{8}\left(\frac{L-L_c}{2}\right)^4+\frac{h^2b_1^2}{24}\left(\frac{L-L_c}{2}\right)^3,\\
&C_{N3}=\frac{2b_1^2}{3}\left[(L-L_c-L_s)^3-\left(\frac{L-L_c}{2}\right)^3\right],\\
&C_{Q3}=\left(\frac{L-L_c}{2}-L_s\right)\left[\frac{2}{3}b_3^2\left(\frac{L-L_c}{2}-L_s\right)^2-\frac{1}{2}(b_2^2+b_3^2)(L-L_c)\left(\frac{L-L_c}{2}-L_s\right)+2b_2^2\left(\frac{L-L_c}{2}\right)^2\right],\\
&C_{M3}=b_3\left(\frac{L-L_c}{2}-L_s\right)^3\left\{\left(\frac{L-L_c}{2}-L_s\right)\left[\frac{b_3}{10}\left(\frac{L-L_c}{2}-L_s\right)-\frac{b_2(L-L_c)}{16}+\frac{b_1h}{32}\right]\right.\\
&\qquad\left.+\frac{L-L_c}{6}\left[-\frac{b_2(L-L_c)}{8}+\frac{b_1h}{8}\right]\right\}+\frac{1}{2}b_2(L-L_c)\left(\frac{L-L_c}{2}-L_s\right)\left\{\frac{b_3}{8}\left(\frac{L-L_c}{2}-L_s\right)^3\right.\\
&\qquad+\frac{1}{3}\left(\frac{L-L_c}{2}-L_s\right)^2\left[b_2(L-L_c)-\frac{b_1h}{2}-\frac{b_3}{8}(L-L_c)\right]+\frac{1}{16}\left(\frac{L-L_c}{2}-L_s\right)(L-L_c)\left[b_2(L-L_c)-\frac{b_1h}{2}\right]\\
&\qquad\left.+\frac{L-L_c}{2}\left[\frac{b_2(L-L_c)}{4}-\frac{b_1h}{4}\right]\left[\frac{L-L_c}{2}-\frac{1}{2}\left(\frac{L-L_c}{2}-L_s\right)\right]\right\}\\
&\quad+b_1\left(\frac{L-L_c}{2}-L_s\right)\left\{\frac{b_3h}{32}\left(\frac{L-L_c}{2}-L_s\right)^3+\frac{1}{3}\left(\frac{L-L_c}{2}-L_s\right)^2\left[-\frac{b_2h(L-L_c)}{4}+\frac{b_1h^2}{8}+\frac{b_3h(L-L_c)}{16}\right]\right.\\
&\qquad-\frac{h}{32}\left(\frac{L-L_c}{2}-L_s\right)(L-L_c)\left[b_2(L-L_c)-\frac{b_1h}{2}\right]\\
&\qquad\left.-\frac{h}{16}(L-L_c)\left[\frac{b_2}{4}(L-L_c)-\frac{b_1h}{4}\right]\left[\left(\frac{L-L_c}{2}-L_s\right)+2(L-L_c)\right]\right\},\\
&C_{N4}=b_3L_s^2\left(\frac{b_3\mu^2L_s}{10}-\frac{\mu}{3}\right)+L_s\left(2-\frac{b_3\mu L_s}{3}\right), \qquad C_{Q4}=\frac{b_3^2L_s^3}{10},\\
&C_{M4}=\frac{1}{2}b_3^2L_s^3\left(\frac{L_s^2}{63}-\frac{h\mu L_s}{36}+\frac{h^2\mu^2}{80}\right),\\
&C_{N5}=L_c, \qquad C_{N6}=L_c,
\end{aligned}
\tag{B.1}
$$

and

$$
\begin{aligned}
&C_{N7}=b_1\left(\frac{L-L_c}{2}\right)^2\left[\frac{1}{3}b_1(L-L_c)-1\right]+\frac{L-L_c}{2}\left[2-\frac{1}{2}b_1(L-L_c)\right], \qquad C_{Q7}=\frac{2}{3}(b_2-c_1)^2\left(\frac{L-L_c}{2}\right)^3,\\
&C_{M7}=\left(\frac{L-L_c}{2}\right)^3\left\{\frac{1}{2}(b_2-c_1)(L-L_c)\left[\frac{(b_2-c_1)}{20}(L-L_c)+\frac{b_1h}{16}\right]+b_1\left[\frac{(b_2-c_1)h}{32}(L-L_c)+\frac{b_1h^2}{24}\right]\right\},\\
&C_{N8}=b_1\left\{\frac{2}{3}b_1\left[(L-L_s-L_c)^3-\left(\frac{L-L_c}{2}\right)^3\right]-\left[(L-L_s-L_c)^2-\left(\frac{L-L_c}{2}\right)^2\right]\right\}\\
&\qquad+2\left(\frac{L-L_c}{2}-L_s\right)-b_1\left[(L-L_s-L_c)^2-\left(\frac{L-L_c}{2}\right)^2\right],
\end{aligned}
$$

$$
\begin{aligned}
C_{Q8} &= \left(\frac{L-L_c}{2}-L_s\right)^2(b_3-c_2)\left[\frac{2}{3}(b_3-c_2)\left(\frac{L-L_c}{2}-L_s\right)-\frac{1}{2}(b_2-c_1)(L-L_c)\right]\\
&\quad -\frac{1}{2}(b_2-c_1)(L-L_c)\left(\frac{L-L_c}{2}-L_s\right)\left[(b_3-c_2)\left(\frac{L-L_c}{2}-L_s\right)-(b_2-c_1)(L-L_c)\right],\\
C_{M8} &= (b_3-c_2)\left(\frac{L-L_c}{2}-L_s\right)^3\left\{\left(\frac{L-L_c}{2}-L_s\right)\left[\frac{b_3}{10}\left(\frac{L-L_c}{2}-L_s\right)-\frac{(b_2-c_1)}{16}(L-L_c)+\frac{b_1h}{32}\right]\right.\\
&\quad \left.+\frac{1}{6}(L-L_c)\left[\frac{(b_2-c_1)}{8}(L-L_c)+\frac{b_1h}{8}\right]\right\}+\frac{1}{2}(b_2-c_1)\left(\frac{L-L_c}{2}-L_s\right)(L-L_c)\\
&\quad \times\left\{-(b_3-c_2)\left(\frac{L-L_c}{2}-L_s\right)^2\left[\frac{1}{8}\left(\frac{L-L_c}{2}-L_s\right)+\frac{1}{12}(L-L_c)\right]+\left(\frac{L-L_c}{2}-L_s\right)\right.\\
&\quad \times\left[\frac{1}{2}(b_2-c_1)(L-L_c)+\frac{b_1h}{4}\right]\left[\frac{2}{3}\left(\frac{L-L_c}{2}-L_s\right)+\frac{1}{4}(L-L_c)\right]+\left[\frac{b_2-c_1}{4}(L-L_c)+\frac{b_1h}{4}\right]\\
&\quad \left.\times\frac{L-L_c}{2}\left[\frac{L-L_c}{2}+\frac{1}{2}\left(\frac{L-L_c}{2}-L_s\right)\right]\right\}+b_1\left(\frac{L-L_c}{2}-L_s\right)\\
&\quad \times\left\{-\frac{(b_3-c_2)h}{32}\left(\frac{L-L_c}{2}-L_s\right)^3-\frac{h}{6}\left(\frac{L-L_c}{2}-L_s\right)^2\right.\\
&\quad \times\left[-\frac{1}{2}(b_2-c_1)(L-L_c)-\frac{b_1h}{4}+\frac{(b_3-c_2)}{8}(L-L_c)\right]+\frac{h}{16}\left(\frac{L-L_c}{2}-L_s\right)(L-L_c)\\
&\quad \left.\times\left[\frac{1}{2}(b_2-c_1)(L-L_c)+\frac{b_1h}{4}\right]+\frac{h}{16}(L-L_c)\left[\frac{b_2}{4}(L-L_c)+\frac{b_1h}{4}\right]\left[\left(\frac{L-L_c}{2}-L_s\right)+2(L-L_c)\right]\right\},\\
C_{N9} &= \frac{b_3^2\mu^2L_s^3}{10},\qquad C_{Q9}=L_s^3b_3\left(\frac{b_3}{10}-\frac{b_2}{4}\right)-L_s^3c_2\left(\frac{b_3}{4}-\frac{2}{3}b_2\right),\\
C_{M9} &= 2b_3^2L_s^3\left(\frac{L_s^2}{252}+\frac{h\mu L_s}{144}+\frac{h^2\mu^2}{320}\right)-2b_3c_2L_s^4\left(\frac{L_s}{36}+\frac{h\mu}{40}\right)+\frac{c_2^2L_s^5}{10}.
\end{aligned}
\tag{B.2}
$$

References

Bao, G., Song, Y., 1993. Crack bridging models for fiber composites with slip-dependent interfaces. J. Mech. Phys. Solids 41, 1425–1444.

Birman, V., Byrd, L.W., 1999. Stiffness of woven ceramic matrix composites with matrix cracks. AIAA-99-1331.

Chou, T.W., Ishikawa, T., 1989. Analysis and modeling of two-dimensional fabric composites. In: Chou, T.W., Ko, F.K. (Eds.), Textile Structural Composites. Elsevier, Amsterdam, pp. 209–264.

Cook, R.D., Young, W.C., 1999. Advanced Mechanics of Materials, second ed Prentice Hall, New Jersey.

Gao, F., Boniface, L., Ogin, S.L., Smith, P.A., Greaves, R.P., 1999. Damage accumulation in woven-fabric CFRP laminates under tensile loading: Part 1. Observations of damage accumulation. Compos. Sci. Tech. 59, 123–136.

Gao, X.-L., Li, K., 2002. Damaged mosaic laminate model of woven fabric composites with transverse yarn cracking and interface debonding. Compos. Sci. Tech. 62, 1821–1834.

Gao, X.-L., Mall, S., 2000. A two-dimensional rule-of-mixtures micromechanics model for woven fabric composites. ASTM J. Compos. Tech. Res. 22, 60–70.

Gao, X.-L., Mall, S., 2001. Variational solution for a cracked mosaic model of woven fabric composites. Int. J. Solids Struct. 38, 855–874.

Gao, Y.-C., Mai, Y.-W., Cotterell, B., 1988. Fracture of fiber-reinforced materials. ZAMP 39, 550–572.

Hashin, Z., 1983. Analysis of composite materials—a survey. ASME J. Appl. Mech. 50, 481–505.

Hashin, Z., 1987. Analysis of orthogonally cracked laminates under tension. ASME J. Appl. Mech. 54, 872–879.

Ji, F.S., Dharani, L.R., Mall, S., 1998. Analysis of transverse cracking in cross-ply composite laminates. Adv. Compos. Mater. 7, 83–103.

McCarty, J.E., Johnson, R.W., Wilson, D.R., 1982. 737 graphite epoxy horizontal stabilizer certification. In: Proceedings of the 23rd AIAA SDM Conference, Part 1, May 1982, New Orleans, LA, pp. 307–322.

Morvan, J.-M., Baste, S., 1998. Effects of two-scale transverse crack systems on the non-linear behaviour of a 2D SiC-SiC composite. Mater. Sci. Eng. A 250, 231–240.

Roy, A.K., 1998a. Variational models for stresses in textile composites and foams. In: Proceedings of the 1998 AFOSR Mechanics of Composite Materials Program Review Meeting, October 14–16, 1998, Dayton, OH, pp. 25–30.

Roy, A.K., 1998b. Comparison of in situ damage assessment in unbalanced fabric composite and model laminate of planar (one-directional) crimping. Compos. Sci. Tech. 58, 1793–1801.

Tan, P., Tong, L., Steven, G.P., 1997. Modelling for predicting the mechanical properties of textile composites—a review. Composites 28A, 903–922.

Tandon, G.P., Pagano, N.J., 1996. Matrix crack impinging on a frictional interface in unidirectional brittle matrix composites. Int. J. Solids Struct. 33, 4309–4326.

Wolfram, S., 1996. The Mathematica Book, third ed Cambridge University Press, Cambridge.